

Wavenumber-resolved turbulence investigations in the ASDEX Upgrade tokamak and comparison to numerical simulations

T. Happel,¹ A. Bañón Navarro,¹ G. D. Conway,¹ C. Angioni,¹ M. Bernert,¹ M. Dunne,² E. Fable,¹ B. Geiger,¹ T. Görler,¹ F. Jenko,¹ R. M. McDermott,¹ F. Ryter,¹ U. Stroth,¹ and the ASDEX Upgrade Team¹

¹Max-Planck-Institute for Plasma Physics, EURATOM Association, 85748 Garching, Germany

²Department of Physics, University College Cork, Association EURATOM-DCU, Cork, Ireland

Introduction

It has been known for several decades that turbulence can lead to energy and particle losses in magnetically confined fusion plasmas. Turbulence can exist in a large interval of characteristic scales ($k_{\perp}\rho_s = 0.1 - 50$, where k_{\perp} is the perpendicular wavenumber of turbulence and ρ_s is the ion gyroradius at electron temperature), which not only causes a loss in confinement, but also has detrimental effects on the way heat loads are deposited on the first wall. Understanding of these turbulence processes is thus not only an academic challenge, but is also important for developing the first wall and the prediction of global plasma behaviour such as confinement, density peaking and intrinsic rotation [1, 2].

In the last 10 years Doppler reflectometry [3, 4] (DR) has evolved into a powerful diagnostic technique using microwave backscattering to measure perpendicular velocities and electron density turbulence levels in magnetic confinement fusion plasmas. The advantages of the scale-dependence of scattering diagnostics and the radial resolution of conventional reflectometry are combined. The Doppler shift of the spectrum of the backscattered wave provides the perpendicular velocity u_{\perp} , the intensity of the Doppler shifted component is proportional to the density fluctuation level \tilde{n}^2 . DR is scale-selective at a chosen k_{\perp} , such that wavenumber spectra and radial turbulence level profiles at different turbulence scales can be obtained by varying k_{\perp} .

Ultimately, a comparison with predictions from numerical turbulence simulations can be used to specifically destabilize a certain instability experimentally. Comparison with experiment provides a benchmark and can help to improve predictive capabilities of numerical simulations in view of future devices such as ITER or DEMO. In this work, a comparison between experiment and numerical simulation is shown. Non-linear GENE [5] simulations have been performed and compared to experimental heat fluxes and turbulence levels.

Diagnostic Setup

A recently installed W-band (75 – 105 GHz) Doppler reflectometer in ASDEX Upgrade (AUG) [6, 7] uses an ellipsoidal mirror to focus the beam to the cutoff-layer. Moreover, the mirror can be rotated to steer the beam, allowing for measurements in a range of perpendicular wavenumbers of turbulence $k_{\perp} = 5 - 25 \text{ cm}^{-1}$. Figure 1 shows a part of a poloidal cross section of AUG (#28245, $t = 2.3 \text{ s}$) with example beam trajectories for different probing beam frequencies (80 and 92 GHz) and mirror angles. At the cutoff-layer the beam is scattered and the antenna receives the $m = -1$ order Bragg backscattering. The spectrum of the backscattered radiation is Doppler shifted, the Doppler shift f_D gives the perpendicular velocity of the plasma

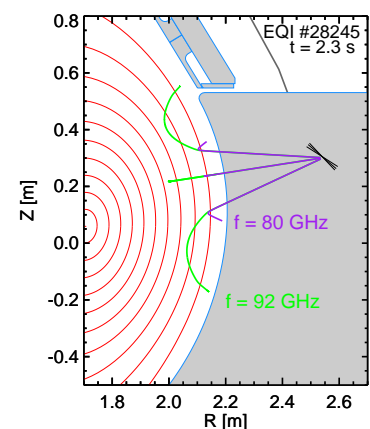


Figure 1: Poloidal cross section of ASDEX Upgrade and probing beam trajectories for different mirror angles.

$2\pi f_D/k_\perp = u_\perp = v_{E \times B} + v_{ph}$, where $v_{E \times B}$ is the $E \times B$ -velocity and v_{ph} is the phase velocity of turbulent density fluctuations. Furthermore, the intensity of the Doppler shifted component is proportional to the density turbulence level $\tilde{n}^2(k_\perp) \propto S(f_D)\Delta f_D$.

Experimental Results

Representative time traces of the discharges presented here are shown in fig. 2. In (a), the constant NBI power at $P_{NBI} = 2.5$ MW is used to establish a base H-mode plasma. Different ECRH power steps (0.5, 1.2, 1.8 MW), deposited at $\rho_{pol} = 0.5$, where ρ_{pol} is the normalized poloidal flux radius, are added. While the line-average density $\langle n_e \rangle$ (b) is roughly constant, the ELM behaviour (c) reacts slightly to the heating changes. At low ECRH power (0.0 and 0.5 MW) the ELMs are smaller and more frequent. In this work, ELM crashes and recoveries have been excluded in the data analysis. In (d), the peripheral electron temperature T_e is shown, where a clear influence of the ECRH heating is observed.

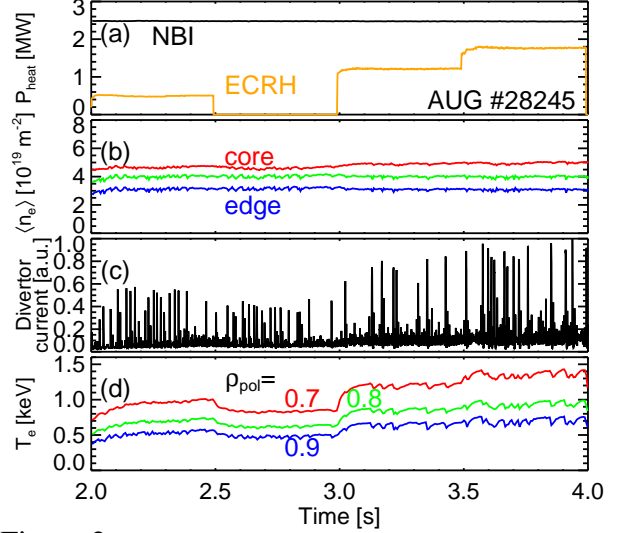


Figure 2: Time traces of (a) heating power, (b) line-average density, (c) ELM monitor and (d) peripheral electron temperature.

Figure 3 shows turbulence levels \tilde{n} for the cases without ECRH ($t = 2.65 - 2.95$ s, blue) and with 1.8 MW additional ECRH power ($t = 3.65 - 3.95$ s, red). Although no absolute values are shown, plots (a-c) can be compared to each other. In (a), \tilde{n} is shown for perpendicular structure scales of $k_\perp = 4 - 8 \text{ cm}^{-1}$. From the core towards the edge, \tilde{n} increases up to roughly $\rho_{pol} = 0.98$, where a significant reduction of turbulence is observed close to the position of the E_r shear layer. The observation is comparable for structure scales $k_\perp = 8 - 13 \text{ cm}^{-1}$, but the turbulence level is in general lower, particularly towards the core. In (c), also an increase in \tilde{n} from core to edge is observed. However, close to the E_r shear layer, no measurements were possible due to a loss of the Doppler shifted component. This might be caused by the fact that in Doppler reflectometry a loss of signal can be observed if the turbulence level falls below a critical value which depends on beam quality, microwave component noise etc. [8, 9].

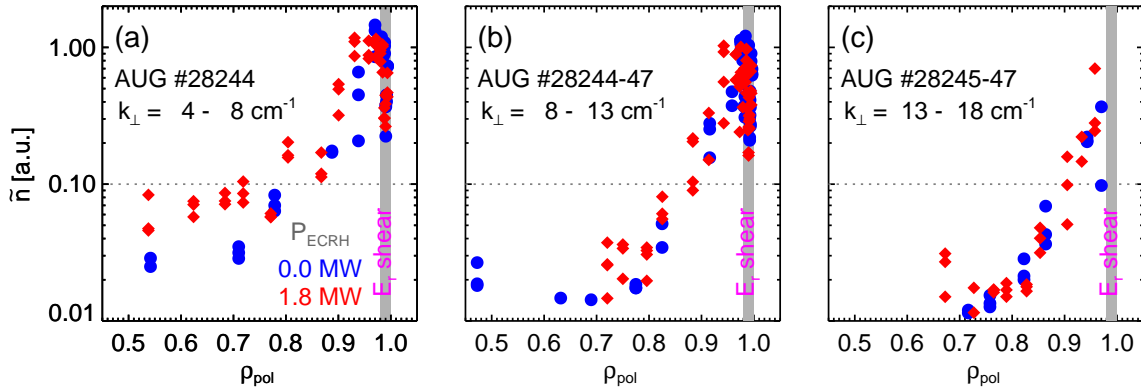


Figure 3: Radial profiles of turbulence level \tilde{n} for different structure scales. An increase in \tilde{n} from core to edge is observed. Close to the E_r shear layer, the turbulence level drops again. At small scales (c), it even drops below the diagnostic limit. The dotted line serves as reference for the eye.

Comparison to ASTRA and GENE results

The solid lines in fig. 4 show experimental ion and electron heat fluxes $Q_{i,e}$ calculated with the ASTRA transport code [10] for the discharge from fig. 2. Note that with $P_{\text{ECRH}} = 1.8$ MW deposited at $\rho_{\text{pol}} = 0.5$, Q_e increases substantially. In this work, non-linear electromagnetic GENE [5] gyrokinetic simulations were performed for scales $k_{\perp}\rho_s \leq 3$ in order to compare heat fluxes to power balance analysis results. The pluses and crosses in fig. 4 are the results from GENE after slight modifications to the input ion-temperature gradient length. For the three outer radii shown, R/L_{T_i} was reduced by 20%. Since ITG modes cause the main heat transport, no changes in R/L_{T_e} have been applied. However, for the (not shown) outer radius at $P_{\text{ECRH}} = 1.8$ MW, small-scale turbulence up to $k_{\perp}\rho_s \sim 80$ could be important, which requires investigating the R/L_{T_e} influence in time-consuming simulations. Moreover, an increased $E \times B$ -shear could reduce the heat flux. Both previous points are under investigation. In general, good agreement is obtained between GENE heat fluxes and the power balance result from ASTRA for the $P_{\text{ECRH}} = 0$ case, while $P_{\text{ECRH}} = 1.8$ MW is still under investigation.

To visualize the above ion temperature gradient length changes necessary to obtain realistic heat fluxes, fig. 5(a) shows the ion temperature profile for the $P_{\text{ECRH}} = 0$ case. Light blue are the measurements from CXRS [11] (10 ms time resolution), while the black circles give the mean of each channel in the time window and error bars are the standard deviation of the

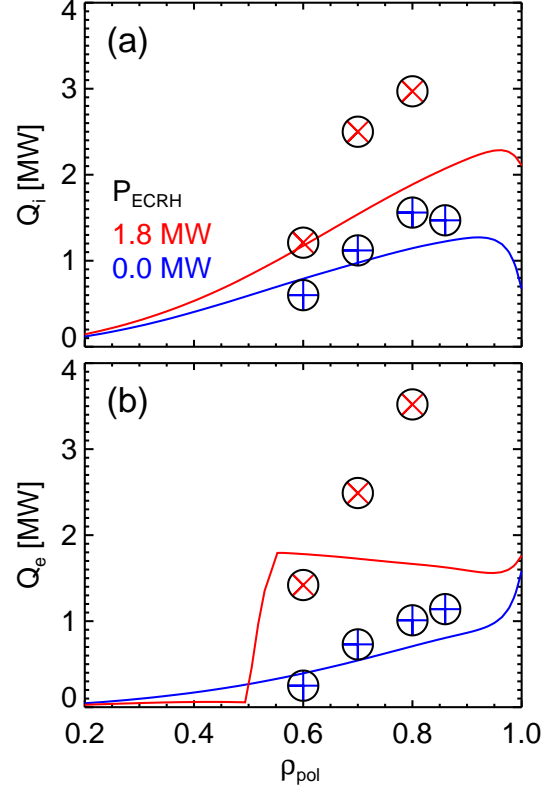


Figure 4: Ion and electron heat fluxes ((a) and (b)). Lines show ASTRA calculations, symbols are non-linear GENE results. For details refer to the text.

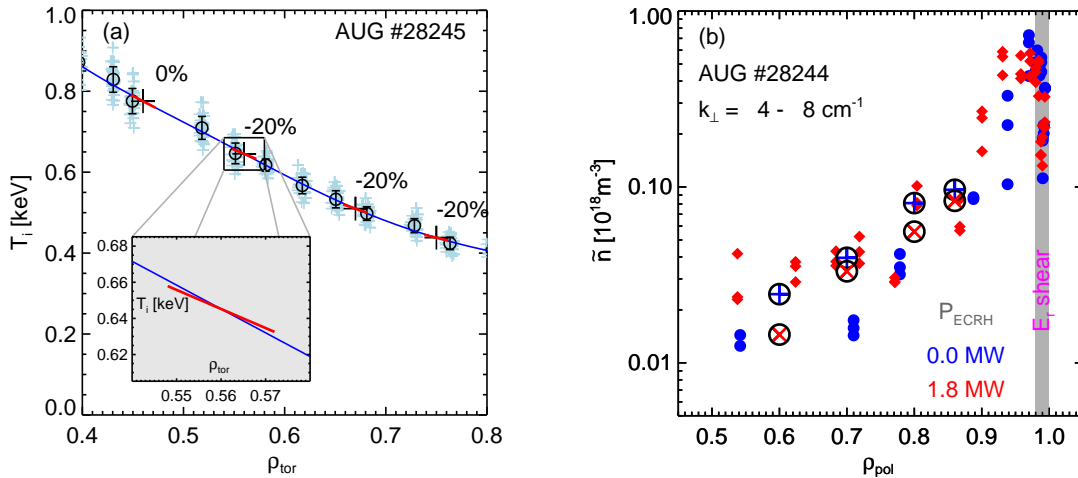


Figure 5: (a) Radial profile of ion temperature. Gradients necessary to achieve experimental heat flux values are shown in red. (b) Comparison of GENE and experimental turbulence levels. Experimental turbulence levels have been scaled by a common factor to match GENE absolute turbulence levels.

respective measurements. The fit to the experimental data is shown in blue, the final GENE input gradients to obtain the heat fluxes from fig. 4, $P_{\text{ECRH}} = 0$, in red. The inset shows a zoom to the radial position $\rho_{\text{tor}} = 0.56$. Locally, a change of -20% in R/L_{T_i} is within the degrees of freedom available to the profile fitting routine. Note that although a change to R/L_{T_i} can be obtained by changing both T_i and ∇T_i , in this work only a change to ∇T_i is considered, since the measurement of the absolute value of T_i is assumed to be more reliable than its gradient.

Figure 5(b) compares the radial turbulence level profile for the largest scales ($k_{\perp} = 4 - 8 \text{ cm}^{-1}$) with results of the GENE simulation (pluses and crosses). The experimental points, which are measured in arbitrary units, have been multiplied by a common factor to give a reasonable match to the absolute \tilde{n} values obtained with the GENE simulation. At first sight, the basic trend measured with Doppler reflectometry, i.e. an increase of turbulence level from core towards edge, is reproduced. However, the GENE simulation with $P_{\text{ECRH}} = 1.8 \text{ MW}$ yields lower turbulence levels than the one with $P_{\text{ECRH}} = 0$, which is in contradiction to the measured values. At the same time, the simulated temperature fluctuations increase, which explains the match to the ASTRA heat fluxes from fig. 4.

Summary

A new Doppler reflectometer has been installed in W-band (75 – 105 GHz) on ASDEX Upgrade which is now working reliably. Owing to its steerable ellipsoidal mirror, the system allows for the measurement of the density turbulence level at different structure scales $k_{\perp} = 5 - 25 \text{ cm}^{-1}$ in a large radial region reaching into the bulk plasma (depending on plasma parameters). In parallel, non-linear GENE simulations have been conducted in order to compare observed heat fluxes and turbulence levels with predictions from gyrokinetic simulation. In general, reasonable agreement is obtained between heat fluxes by varying the input gradients R/L_{T_i} only slightly (up to 20%). The radial turbulence level profile shows agreement in its general trend – an increase from plasma core towards the edge – but a discrepancy is found in the plasma response to additional ECRH heating: while the Doppler reflectometry turbulence level increases, the one from GENE decreases. Both scans in R/L_{T_e} and the $E \times B$ -shear are ongoing work in order to clarify these points.

References

- [1] E. Doyle *et al.*, Nucl. Fusion **47**, S18 (2007).
- [2] C. Angioni *et al.*, Phys. Rev. Lett. **107**, 215003 (2011).
- [3] X. L. Zou *et al.*, *Poloidal Rotation Measurement in Tore Supra by Oblique Reflectometry* (Proc. 4th International Reflectometry Workshop, Cadarache, France, 1999), report EUR-CEA-FC-1674.
- [4] M. Hirsch *et al.*, *Doppler Reflectometry for the Investigation of poloidally propagating Density Perturbations* (Proc. 4th International Reflectometry Workshop, Cadarache, France, 1999), report EUR-CEA-FC-1674.
- [5] F. Jenko *et al.*, Phys. Plasmas **7**, 1904 (2000).
- [6] C. Tröster, Ph.D. thesis, Ludwig-Maximilians-Universität München, 2008.
- [7] T. Happel *et al.*, *Design of a new Doppler Reflectometer Front End for the ASDEX Upgrade Tokamak* (Proc. 10th International Reflectometry Workshop, Padua, Italy, 2011).
- [8] G. D. Conway, Plasma Phys. Control. Fusion **41**, 65 (1999).
- [9] G. D. Conway *et al.*, Plasma Phys. Control. Fusion **46**, 951 (2004).
- [10] G. Pereverzev *et al.*, Technical Report No. IPP 5/98, Max-Planck Institute.
- [11] R. M. McDermott *et al.*, Plasma Phys. Control. Fusion **53**, 124013 (2011).